

Visualizing Local Minima in Multi-Robot Motion Planning using Morse Theory

Andreas Orthey¹ and Marc Toussaint^{1,2}

¹ Max Planck Institute for Intelligent Systems, Stuttgart, Germany
aorthey@is.mpg.de

² University of Stuttgart, Germany

Abstract. Multi-robot motion planning problems often have many local minima. It is essential to visualize those local minima such that we can better understand, debug and interact with multi-robot systems. Towards this goal, we use previous results combining Morse theory and fiber bundles to organize local minima into a local minima tree. We extend this local minima tree to multi-robot systems by introducing fiber bundle diagrams and devising a new algorithm to compute, project and sample from fiber bundles. We demonstrate this algorithm on several multi-robot systems of up to 20 degrees of freedom.

Keywords: Multi-robot motion planning, Morse Theory, Fiber bundles, Visualization of Local Minima

1 Introduction

Coordinating multiple robots is essential to automate surveillance of climate changes, to collaborate on construction sites and to route autonomous vehicles. Problems of coordinating multiple robots often involve many local minima. Existing algorithms, however, usually do not explicitly visualize those local minima and often return only a single optimal solution [10].

To solve multi-robot motion planning problems, we argue it to be essential to visualize local minima. By visualizing local minima, we can obtain conceptual understanding about the underlying topological complexity [22], extract symbolic representations [28] and analyse the convergence of optimization algorithms [34]. By visualizing local minima, we allow interaction by non-expert users, to either guide or prevent motions [17]. By visualizing local minima, we can create high-level options [18], usable to make high-level decisions [25] or perform rapid re-planning [32].

Visualizing local minima is therefore an important requirement for multi-robot motion planning. To enumerate local minima, we develop a new algorithm we call the *multi-robot motion explorer*. The explorer extends previous works on single-robot motion planning [17]. In particular, we evoke Morse theory [14] to enumerate local minima. To each local minimum we assign an equivalence class of paths converging, under optimization, to the same local minimum. Using those equivalence classes, we use fiber bundles [16] to organize local minima into a

local-minima tree. Eventually, non-expert users can interact with this tree by navigating through it similar to navigating through a unix filesystem.

Our contributions are

1. Extension of fiber bundles [16] to composite configuration spaces by introducing fiber bundle diagrams
2. Extension of explorer algorithm [17] to multi-robot systems and implementation in the Open Motion Planning Library (OMPL) [26]
3. Demonstration of algorithm on six multi-robot planning problems of up to 20 degrees of freedom

2 Related Work

To visualize local minima, we need to solve two associated problems. First, we need to find a representation of the configuration space. Second, we need to utilize this representation to extract local minima.

2.1 Multi-Robot Motion Planning

To represent a multi-robot motion planning problem, we can consider the robots as one generalized robot under robot-robot collision constraints in a composite configuration space [10]. In general, we can use such an approach only for a few low-dimensional robots, mainly because the problem itself is NP-hard [8]. Since the problem is NP-hard, it becomes necessary to reduce the composite configuration space. Depending on the type of robots, we can group reduction methods into two classes.

First, we have reductions for the case where all robots are equivalent (homogeneous). For homogeneous multi-robot systems, we can project all start and goal configurations onto the configuration space of the first robot and find a graph connecting all configurations. To coordinate the motion of the robots along that graph we need to solve the pebbles-on-a-graph problem, which we can solve efficiently [9], either by converting it to an integer linear program [33], by partitioning the graph into regions densely or sparsely connected [20] or by utilizing simple push and swap strategies [11]. By utilizing solvers for pebbles-on-a-graph, we can for example create a larger framework to compute motions for swarms of drones [7].

Second, we have reductions for the case where robots are not equivalent (non-homogeneous). For non-homogeneous multi-robot systems, we can first compute graphs on each individual configuration space and then merge them into a graph on the composite configuration space [10]. To merge graphs, we can either use path coordination or graph coordination.

In path coordination [21], we compute paths for each robot separately. We then coordinate the execution of those paths, either by searching over the space of reparameterizations [21] or by prioritizing the robots [5].

In graph coordination, we compute graphs for each robot separately. We then combine the graphs into an (implicit) composite configuration space graph [27]. To compute this graph, we can use two methods.

First, we can create the *tensor product* of graphs, whereby all edges are combined [24]. To explore the tensor product, we can either use a random search utilizing a direction-oracle [24] or we can execute shortest paths optimistically until conflicts arise. When conflicts arise, we can expand locally the dimensionality to resolve conflicts [30]. We can combine both methods using prioritization of robots, for example by analyzing possible start and goal conflicts [29] or by the number of topologically varying paths a robot can execute [31].

Second, we can create the *cartesian product* of graphs, whereby only edges are used where at most one robot moves. We can think of the cartesian product as an approximation to the tensor product, in the sense that every multi-robot path can be arbitrarily close approximated by a path where at most one robot moves at a time [27]. However, if the underlying graphs are not dense enough, we can miss valid paths and thereby sacrifice completeness.

It is important to note that non-homogenous and homogenous robots are not mutually exclusive, but we can often further simplify non-homogenous robot problems by decomposing them into problems of groups of homogenous robots [23].

2.2 Multi-Path Multi-Robot Motion Planning

From a given representation of the composite configuration space, we like to extract local minima. Local minima can often be defined as representative paths of equivalence classes, where we define an equivalence relation on the path space for the purpose of grouping paths. Grouping paths can be done using different approaches, of which we discuss three fundamental ones.

First, we can group paths topologically [15]. In a topologically grouping, we use the notion of homotopy to define two paths to be equivalent if they can be continuously deformed into each other. To find paths which differ homotopically, we can compute a simplicial complex of the configuration space and extract paths [19] or by computing an H-score determining the number of times a path crosses subsets of the configuration space [2].

Second, we can group paths based on braid patterns [1]. In a braid pattern grouping, we define two paths to be equivalent if pairwise robot crossings are equivalent. By ignoring the type of crossing, we obtain a permutation group of robots. Using this permutation group, we can compute representative paths of varying braid pattern [12]. We can alternatively find paths of varying braid pattern by planning a minimal-cost path constrained to a pattern [13] or by following a braid pattern controller, for example with safety separations [3].

Third, we can group paths based on Morse theory [14]. In Morse theory, we define two paths to be equivalent if they converge, under optimization, to the same local minimum [17]. This differs from braid theory and topology (1) by being finer in the sense that two equivalent paths under braid theory or topology can converge to two different minima, (2) by being defined relative to an

optimizer and (3) by being often more computationally efficient in higher dimensions. In previous work we used Morse theory in single-robot motion planning [17]. In this work, we generalize this approach to multi-robot motion planning.

3 Foundations

Let r_1, \dots, r_M be M robots with associated *component* configuration spaces Y_1, \dots, Y_M of dimensionality n_1, \dots, n_M . We define the (composite) configuration space $X = Y_1 \times \dots \times Y_M$ of dimensionality $n = n_1 + \dots + n_M$. The space of constraint-free configurations is denoted as X_f . The motion planning problem (X_f, x_I, x_G) asks us to find a path from a start configuration $x_I \in X_f$ to a goal configuration $x_G \in X_f$.

The space of solutions to the motion planning problem is given by the associated path space. The path space P_f is the space of all continuous paths $p : I \rightarrow X_f$ on X_f starting at x_I and ending at x_G . To analyse P_f , we enumerate local minima using Morse theory and use fiber bundles to organize the local minima into a local minima tree.

3.1 Morse Theory

We utilize Morse theory [14] to identify local minima. A local minimum is an invariant of the path space P_f under optimization of a cost functional. A cost functional J maps a path $p \in P_f$ to a real number \mathbb{R} as

$$J[p] = \int_0^1 L(x, p(x), p'(x)) dx \quad (1)$$

whereby L is a loss term. To solve Eq. 1, we can take one of two views. In the first view, we interpret Eq. (1) as a problem of optimal control or calculus of variation in the small [6], where we like to find *one* global minimal solution. In the second view, however, we interpret Eq. (1) as a problem of Morse theory or calculus of variation in the large [14], where we like to find *all* local minimal solutions.

In this paper, we adopt the Morse theoretic view to enumerate local minima. We define a local minimum as an invariant of Eq. (1) under optimization. To optimize, we use a local optimizer $\Phi_J : P_f \rightarrow P_f$ which we assume to be given. We require Φ_J to be different from an identity mapping, but make no other assumption about its behavior.

Following Morse theory, we interpret the optimizer Φ_J as an equivalence relation³ on the path space [17]. In particular, given two paths $p, p' \in P_f$ we define them to be equivalent, written as $p \sim_{\Phi_J} p'$, if $\Phi_J(p) = \Phi_J(p')$. We then take the quotient $Q = P_f / \sim_{\Phi_J}$ which represents equivalence classes of paths under

³ Recall that an equivalence relation \sim on a path space P is a binary relation such that for any paths $a, b, c \in P$ we have $a \sim a$ (Reflexive), if $a \sim b$ then $b \sim a$ (Symmetric) and if $a \sim b$ and $b \sim c$ then $a \sim c$ (Transitive) [15].

optimization. Each equivalence class will be *represented* by one path invariant under optimization, i.e. a *local minimum* p^* for which we have $\Phi_J(p^*) = p^*$. Under this representation, we associate to every X_f its local-minima space Q containing all local-minima of P_f .

3.2 Fiber Bundles

Finding and interpreting local minima is often too difficult in high-dimensional configuration spaces. To simplify those spaces, we utilize sets of admissible lower-dimensional projections, which we model as fiber bundles. Fiber bundles are both useful to decrease planning time [16] and to group local minima into more meaningful classes [17].

A fiber bundle is a tuple (X, F, B) which consists of mappings

$$F \rightarrow X \rightarrow B \quad (2)$$

whereby X is the bundle space, F is the fiber space, B the base space, $F \rightarrow X$ is the inclusion map, and $\pi : X \rightarrow B$ is the projection map. We require the projection map to be admissible, meaning that if X_f is the free space of X and B_f is the free space of B , then X_f is a subset of $\pi^{-1}(B_f)$ [16]. Informally, it means that we require every path in X_f to project onto B_f . If paths do not project onto B_f we might remove valid local minima. We will often abbreviate an admissible fiber bundle using the shorthand $X \xrightarrow{\pi} B$.

Remark on Admissibility In practice, we compute admissible projections by removing links, removing robots or by nesting simpler robots with less degrees-of-freedom.

3.3 Local-Minima Tree

By combining Morse theory and fiber bundles, we can organize local minima into a local minima tree. Let $X \xrightarrow{\pi} B$ be a fiber bundle. If Q is the space of local minima associated with X_f , we can reduce Q by introducing the notion of projection-equivalence. Two paths $q, q' \in Q$ are said to be projection-equivalent, written as $q \sim_{\{\Phi_J, \pi\}} q'$, if $\Phi_J(\pi(q)) = \Phi_J(\pi(q'))$. Taking the quotient of Q with respect to projection-equivalence results in the quotient $Q_B = Q / \sim_{\{\Phi_J, \pi\}}$. If we have a sequence of fiber bundles $X_K \xrightarrow{\pi_K} X_{K-1} \xrightarrow{\pi_{K-1}} \dots \xrightarrow{\pi_1} X_0$ with $X_K = X$, we can iteratively apply projection-equivalence to obtain a sequence of local-minima spaces Q_K, Q_{K-1}, \dots, Q_0 [17].

The sequence of local minima spaces can be grouped into a local-minima tree. The tree $T_{1:K} = (V, E)$ consists of local minima as vertices V and directed edges E , whereby an edge exists between vertex v and vertex v' if the local minimum v' is equivalent, after projection, to v .

4 Method

We previously used local-minima trees to visualize local minima of single-robot motion planning problems [17]. Here, we discuss the changes required to visualize local minima of multi-robot motion planning problems. We develop three extensions. First, we present fiber bundle diagrams, a tool to better interpret and visualize fiber bundles. Second, we extend the explorer algorithm [17], which finds local minima trees by computing paths on sparse graphs. Third, we discuss the changes to our implementation in the Open Motion Planning Library (OMPL).

4.1 Fiber-Bundle Diagram

While fiber bundles are useful reduction tools, they can be too cumbersome to understand, in particular in multi-robot scenarios. To better understand and visualize fiber bundles, we develop the *fiber bundle diagram*. The fiber bundle diagram is a representation of a fiber bundle sequence $X_K \xrightarrow{\pi_K} \dots \xrightarrow{\pi_1} X_0$. In particular, using the diagram, we can visualize which part of the bundle space is projected onto which part of the base space and we can visualize the size and type of the fiber space.

To construct the fiber bundle diagram, we draw a diagram consisting of four rectangle types (see Fig. 1a). First, we represent the full bundle space on the bottom of the diagram (grey rectangle). Second, we show projections of the bundle space onto the base space (hatch patterned rectangle). Third, the base space is shown on top of the bundle space (grey rectangle), which becomes the bundle space for the next level. Fourth, we show the fiber space (dashed, white rectangle).

For multiple robots, we divide the bundle space into components, one component for each robot. For each component, we define the length of each rectangle to be equivalent to the number of dimensions.

As an example, we show real fiber bundle diagrams in realistic multi-robot scenarios. First, Fig. 1b shows the reduction for a two-drone system, where we first reduce both drones from their bundle space $SE(3)$ to the base space \mathbb{R}^3 representing a spherical ball inscribed into the drone. On the next level we then remove the second ball which represents a projection from $\mathbb{R}^3 \times \mathbb{R}^3$ onto \mathbb{R}^3 . Note that the same diagram could be written formally as $SE(3) \times SE(3) \rightarrow \mathbb{R}^3 \times \mathbb{R}^3 \rightarrow \mathbb{R}^3$, but that would hide the important information of which parts of the bundle space are mapped onto which parts of the base space. Furthermore, we can quickly read out the size and type of the fiber.

The other fiber diagrams show a reduction for three disks on a square (Fig. 1c), three disks in a tee (Fig. 1d), two mobile manipulators crossing (Fig. 1e) and two manipulators with one drone (Fig. 1f), respectively.

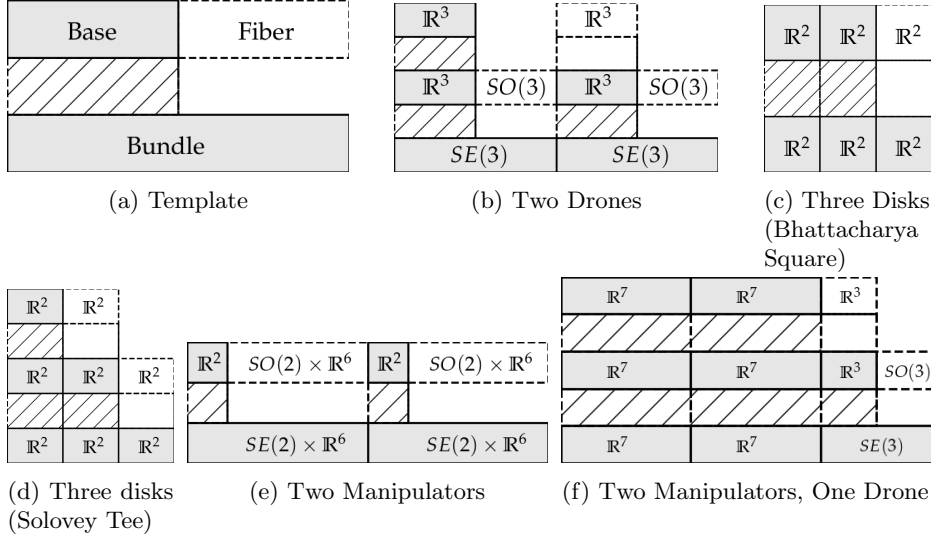


Fig. 1: Fiber bundles reductions represented by fiber bundle diagrams. *Gray rectangles*: Base or Bundle spaces, *White and dashed rectangles*: Fiber spaces, *Hatch patterned rectangles*: Projections from Bundle to Base space.

4.2 Multi-robot motion explorer

We use the fiber bundle diagrams to extend the single-robot motion explorer algorithm [17]. We first give a brief summary of the motion explorer and then discuss the necessary extensions.

Single-robot motion explorer In the single-robot motion explorer algorithm, we take as input a planning problem (X_f, x_I, x_G) , a prespecified fiber bundle $X_K \xrightarrow{\pi_K} X_{K-1} \xrightarrow{\pi_{K-1}} \dots \xrightarrow{\pi_1} X_0$, a cost functional J and an optimizer Φ_J . To each bundle space X_k we associate a dense graph \mathbf{G}_k and a sparse graph \mathbf{S}_k . We then compute local minima in six steps.

First, we compute the associated fiber spaces by taking the quotient $F_k = X_{k+1}/X_k$. Second, we project x_I and x_G onto the base spaces. Third, we let the user pick a local minimum q_k . Fourth, we compute a dense graph \mathbf{G}_{k+1} on X_{k+1} by sampling the graph \mathbf{G}_k , biased towards the local minimum q_k , and by concatenating it with a sample from the fiber space F_k . Fifth, we extract a sparse subgraph graph \mathbf{S}_k from \mathbf{G}_k using a graph reduction method [4]. Sixth, we enumerate up to N paths by searching N -shortest paths on the sparse graph \mathbf{S}_k using a depth-first search method and let them converge to a local minimum using optimizer Φ_J [17]. Finally, we add a minimum to the tree if it cannot be straight-line deformed into an existing minimum. We then display the local minima tree to the user.

Algorithm 1 ComputeFiberSpace(X_k, X_{k+1})

```

1:  $Y_{1:M}^k \leftarrow \text{GETCOMPONENTSPACES}(X_k)$ 
2:  $Y_{1:M}^{k+1} \leftarrow \text{GETCOMPONENTSPACES}(X_{k+1})$ 
3: for each  $Y_m^k$  in  $Y_{1:M}^k$  do
4:    $F_m^k \leftarrow Y_m^{k+1} / Y_m^k$ 
5: end for
6:  $F_k \leftarrow \text{FLATTEN}(F_{1:M}^k)$ 
7: return  $F_k$ 

```

Algorithm 2 ProjectOntoBase(x_{k+1}, X_{k+1}, X_k)

```

1:  $x_k^{1:M} \leftarrow \text{SPLITINTOCOMPONENTS}(x_{k+1}, X_{k+1})$ 
2:  $Y_{1:M}^k \leftarrow \text{GETCOMPONENTSPACES}(X_k)$ 
3: for each  $x_{k+1}^m$  in  $x_{k+1}^{1:M}$  do
4:    $x_k^m \leftarrow \text{PROJECT}(x_{k+1}^m, Y^k)$ 
5: end for
6:  $x_k \leftarrow \text{FLATTEN}(x_k^{1:M})$ 
7: return  $x_k$ 

```

Algorithm 3 SampleBundleSpace($\mathbf{G}_k, q_k, F_k, X_k, X_{k+1}$)

```

1:  $x_k^{1:M} \leftarrow \text{SAMPLEBASE}(\mathbf{G}_k, q_k, X_k)$ 
2:  $x_{F_k}^{1:M} \leftarrow \text{SAMPLEFIBER}(F_k)$ 
3:  $Y_{1:M} \leftarrow \text{GETCOMPONENTSPACES}(X_{k+1})$ 
4:  $x_{k+1}^{1:M} \leftarrow \text{ALLOCATECOMPONENTCONFIGURATIONS}(Y_1, \dots, Y_M)$ 
5: for each  $Y_m$  in  $Y_1, \dots, Y_M$  do
6:    $x_{k+1}^m \leftarrow \text{CONCAT}(x_k^m, x_{F_k}^m, Y_m)$ 
7: end for
8:  $x_{k+1} \leftarrow \text{FLATTEN}(x_{k+1}^{1:M})$ 
9: return  $x_{k+1}$ 

```

Extensions to multiple robots To extend the single-robot motion explorer algorithm to multi-robot planning problems, we develop four extensions.

First, we compute the fiber space by following the reduction in the fiber diagram (Alg. 1). In particular, we get the component spaces for base and bundle space (Line 1,2), then compute fibers for each component individually (Line 4) and combine them into one generalized fiber space (Line 6).

Second, we change the projection operator from bundle to base space (Alg. 2). In particular, we take a configuration $x_{k+1} \in X_{k+1}$, split it into its components (Line 1), and project each component onto the individual component base spaces (Line 4). We then combine all projected configurations into the generalized base space configuration (Line 6).

Third, we extend the fiber bundle sampling method (Alg. 3). To sample a configuration x_{k+1} on X_{k+1} , we sample a configuration x_k on X_k by sampling from the dense graph \mathbf{G}_k biased towards the local minimum path q_k (Line 1). We then sample a configuration x_{F_k} uniformly on the fiber space F_k (Line 2). Both

configurations are split into its components. We then allocate a new configuration x_{k+1} , split into components $x_{k+1}^{1:M}$ (Line 4). We then concatenate component configurations x_k^m and $x_{F_k}^m$ to obtain a component configuration x_{k+1}^m (Line 6). Finally, we flatten the component configurations into x_{k+1} (Line 8) and return the configuration (Line 9). Note that the `Flatten` operation is done implicitly in the code, where we only manipulate references to the components of each configuration.

Fourth, we add two additional projection operators. The first operator is an empty-set projection $Y_m \rightarrow \emptyset$, which we use to remove a complete robot. The second operator is an identity projection $Y_m \rightarrow Y_m$, which we use to copy a component configuration space without changes. Both operators are not necessary in the single-robot case, but they become essential for multiple robots, where we often like to simplify the problem by removing certain robots while keeping the remaining ones unchanged.

4.3 Implementation Details

We provide an implementation of the multi-robot motion explorer algorithm in C++, which is freely available⁴ and utilizes the Open Motion Planning Library (OMPL) [26].

Compared to our previous single-robot implementation [17], we additionally implement two minor extensions. First, we change the visualization of the local minima tree by utilizing only straight line elements to make it better readable. Second, we extend the visualization of paths to multi-robot systems by visualizing the trace of a point on each component robot during the path execution. The points mark end-effector positions, tool-center points or geometric centers of a robot. Each trace is then annotated by an arrow showing the movement direction.

5 Demonstrations

To show the applicability of the multi-robot motion explorer, we demonstrate it on a variety of multi-robot systems. We execute all demonstrations on a laptop with a four-core 2.5GHz processor, 8GB Ram running Ubuntu 16.04. We use the same parameters as for the single-robot case [17].

Remark on Demonstrations For each demonstration, our task is to visualize local minima which move the robots from an initial configuration in green to a goal configuration in red⁵. We first grow a graph for a time budget t_b , then we enumerate and verify local minima and report on the time and number of

⁴ github.com/aorthy/MotionPlanningExplorerGUI

⁵ If printed in greyscale, initial configuration is in lightgrey, goal configuration in darkgrey and robot during execution in white.

local minima found. Note that the times reported are rough estimates depending on the underlying sampling process and the chosen local minima. For each demonstration, we assume that a fiber bundle is pre-specified. The ones chosen are shown in Fig. 1, which we picked due to faster computation time and leading to more meaningful local minima for users of the system.

Crossing Disks (2-dof) The crossing disk problem involves two disks labeled 1 and 2, which can each move on orthogonal line segments (Fig. 2). The disks are not allowed to collide, creating a two-dimensional configuration space containing a circular hole in the middle (Fig. 2a). Our algorithm finds two local minima after 0.47s ($t_b = 0.1$ s), which we label p_1 and p_2 , respectively. When choosing minimum p_1 , disk 1 goes first and disk 2 follows (Fig. 2b). On minimum p_2 , disk 2 goes first and disk 1 follows (Fig. 2c).

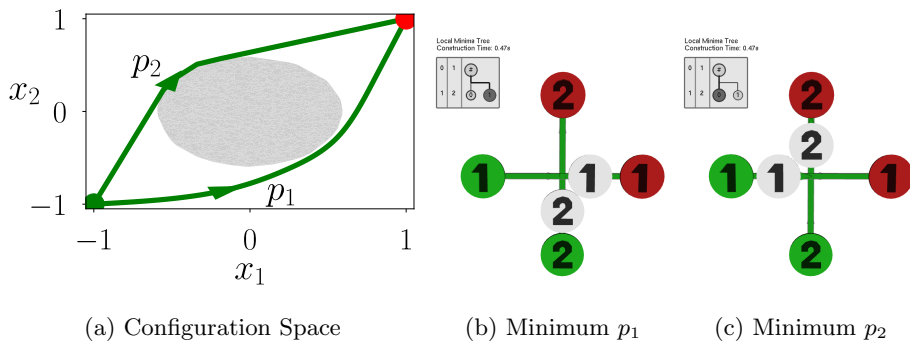


Fig. 2: Visualizing two local minima for the crossing of two disks.

Solovey Tee (6-dof) We next visualize local minima for three disks in a tee, a scenario proposed by Solovey et al. [24] (Fig. 3a). In this scenario, local minima depend on the right fiber bundle. To see this, we use two different fiber bundles, one where we first remove disk 3 and then remove disk 2 (non-optimal) and one where we first remove disk 1 and then remove disk 2 (optimal). For the optimal fiber bundle, we find one local minimum each in 0.21s, 0.30s and 3.07s ($t_b = 0.2$ s), respectively (Fig. 3b). On the minimum, disk 3 goes straight towards the goal, while disk 1 and 2 clear the path by moving into the aisle. For the non-optimal fiber bundle, however, we find two local minima requiring 0.22s, 0.43s and 25.72s, respectively (Fig. 3c). Both local minima are similar in that disks 1 and 2 first move towards the goal, let disk 3 pass into the aisle, then move backwards to let disk 3 pass towards the goal.

Drones on a Tree (12-dof) We next visualize local minima for two drones flying around a tree (Fig. 4a). The fiber bundle reduction is given in Fig. 1b.

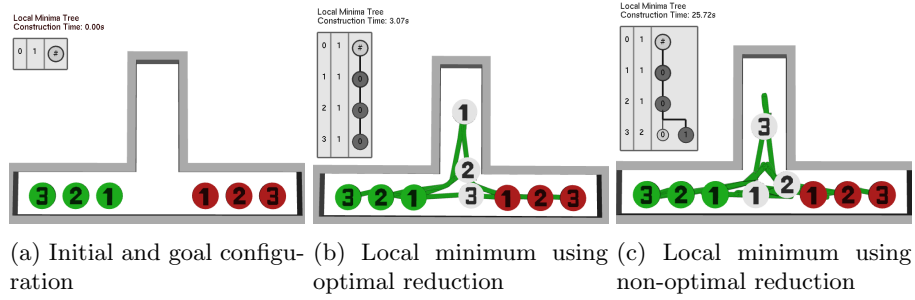


Fig. 3: Three disks in a tee (Solovey et al. [24])

We find five local minima for the first drone reduction in 5.5s ($t_b = 0.1s$). We then select the path going left around the tree, find three minima in 2.05s for the second drone (Fig. 4b) and finally compute a valid local minimum in 0.19s where both drones fly left around the tree (Fig. 4c).

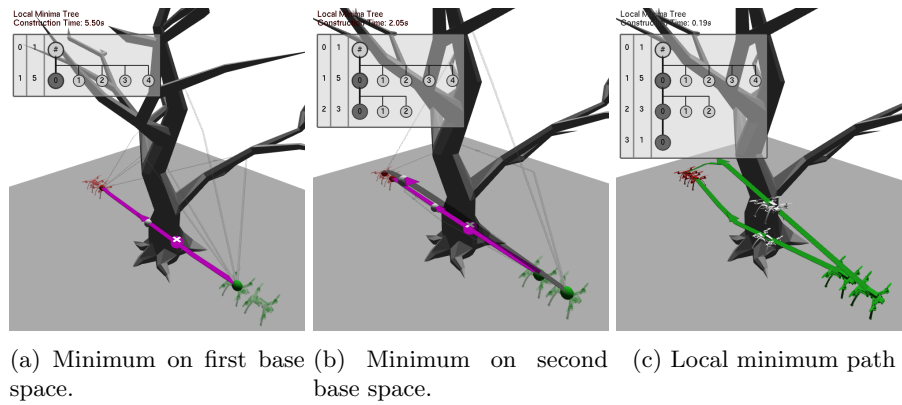


Fig. 4: Two drones flying around a tree.

Two-Arm Manipulator Baxter (14-dof) We next visualize local minima for the two-arm Baxter robot. We consider each arm as a separate fixed-base manipulator of 7-dofs. The composite configuration space has 14 dimensions. We consider a problem where Baxter has both arms in front of its torso with the left arm on top (Fig.5a). The goal is to change the position of the arms, such that the right arm is on top. We find two local minima in 13.64s ($t_b = 10s$) planning time. On the first local minimum, the left arm is moved backward and down (Fig.5b), on the second local minimum, the left arm is moved forward and down (Fig.5c).

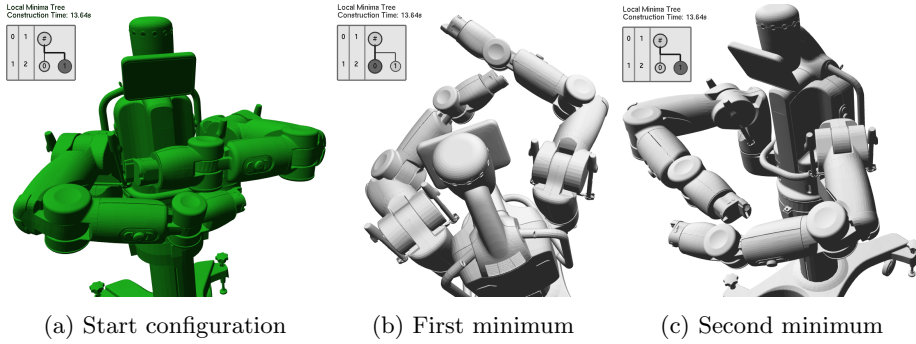


Fig. 5: Visualizing local minima for 14-dof baxter robot.

Manipulators Crossing (18-dof) We next visualize local minima for two mobile manipulators which need to cross each other to reach their goal (Fig. 6). The composite configuration space is 18 dimensional. We use a reduction onto the base of the robots which is equivalent to two disks crossing. After planning for 0.57s ($t_b = 0.3s$) we find two local minima corresponding to the left manipulator going first or the right manipulator going first (Fig. 6a). Choosing the right manipulator to go first, we then compute three local minima in 2.38s on the composite configuration space, which correspond to different rotations of the arms (Fig. 6b and 6c).

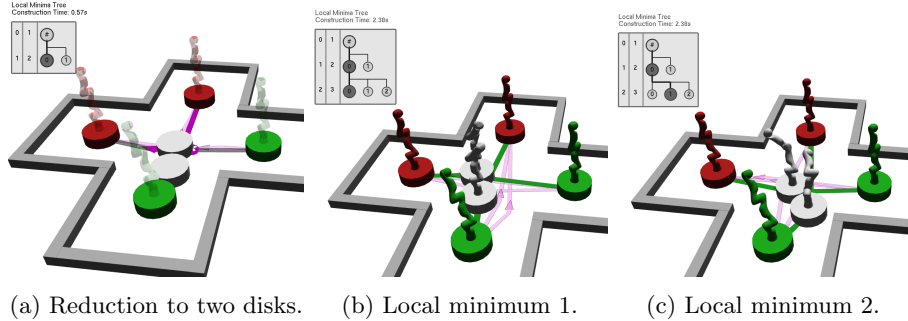


Fig. 6: Two manipulators navigating a crossing.

Drone Crossing Manipulators (20-dof) We next visualize local minima for a drone crossing through two fixed-base manipulator arms which have to change places (Fig. 7a). The composite configuration space has 20 dimensions. The fiber bundle reduction is shown in Fig. 1f. On the lowest dimensional base space (14 dimensions), we compute 5 local minima in 8.96s ($t_b = 1s$), whereby two minima

correspond to the forward/backward motions as in the Baxter demonstration. The other minima are variations of those but with additional rotations of the joints. We then use the local minimum where the right manipulator passes behind the left manipulator to compute in 2.15s two local minima for the inscribed sphere of the drone, one going above (Fig. 7b), one going below the right manipulator. We use the local minima going above the right manipulator to obtain four minima in 26.36s on the bundle space (Fig. 7c). Those minima correspond to different rotations of the drone when flying above the manipulator.

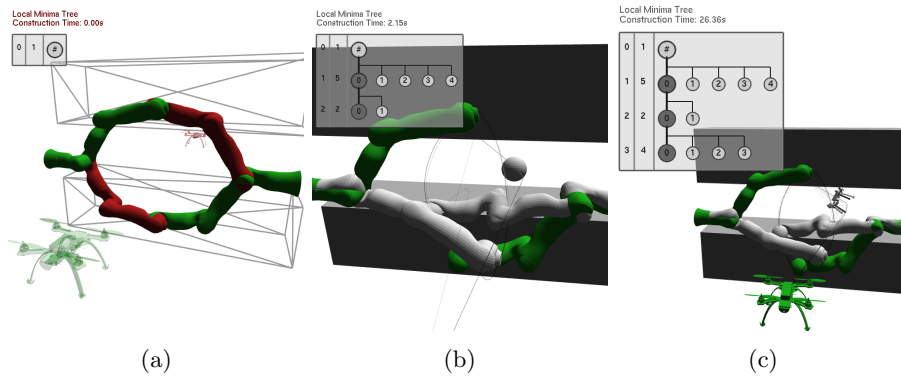


Fig. 7: Visualizing local minima for a drone flying through two fixed-base manipulators.

Bhattacharya Square (6-dof) This scenario involves three labeled disks on a unit square [2] (Fig. 8). Following the discussion by Bhattacharya and Ghrist [2], this scenario involves at least eight non-winding homotopy classes. We can obtain a meaningful grouping by removing the third disk. In that case we have two local minima depending on if disk 1 goes first or disk 2 goes first. Our algorithm finds both minima in 2.65s ($t_b = 0.3s$). As can be seen in Fig. 8a, we find four local minima, two being slight variations of the desired local minima. This can be due to premature convergence of the optimizer or intricate geometric features in 4-d space. We then select the minimum where disk 2 goes first and find in 6.15s three local minima on the bundle space. By inspection, we know that there should be four minima depending on if disk 3 goes before or after disk 1 and before or after disk 2. However, we only find the minimum where disk 3 goes before disk 1 and before disk 2 (Fig. 8b) and the minimum where disk 3 goes before disk 2 and after disk 1 (Fig. 8c). We do not find the other local minima, most likely because they belong to narrow passages in the configuration space. We occasionally observe the algorithm to find local minima with cycling behavior, where two robots meet, cycle around each other and then continue onward. We discuss possible solutions to those problems in Sec. 6.

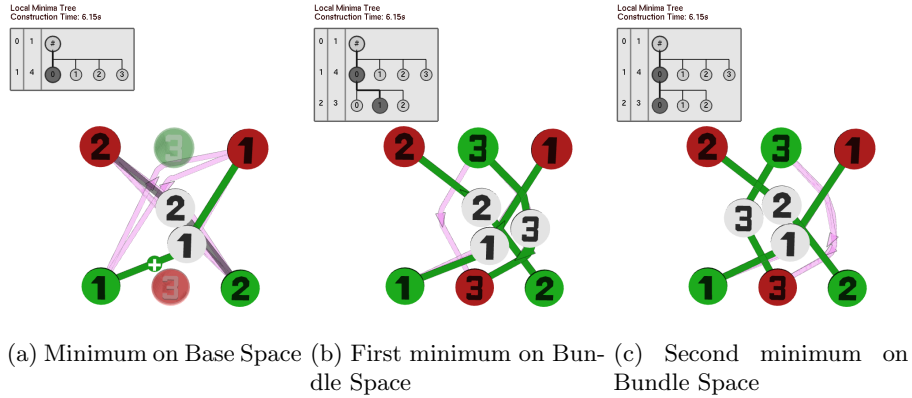


Fig. 8: Three labeled disks on a square (Bhattacharya and Ghrist [2]).

6 Conclusion

To visualize local minima, we developed the multi-robot motion explorer. Using the explorer, we extended previous results on single-robot visualization [17] by introducing fiber bundle diagrams and extending the sampling functions of the explorer. In demonstrations, we showed the explorer to be applicable to several multi-robot scenarios involving disks, drones, and manipulator arms.

While the algorithm works robustly on many robot platforms, we observed three limitations. First, we often missed local minima when the configuration space contained narrow passages. We could alleviate this problem by biasing sampling towards narrow passages, by analyzing locally reachable sets [25] or by targeted sampling of undiscovered braid pattern [3]. Second, the algorithm can return minima with cycling behavior, where two robots cycle around each other before continuing. We could alleviate this problem by detecting and removing cycles or by penalizing cycle paths using additional cost functionals. Third, we rely on manually specified fiber bundle reductions. To automate this, we could specify a set of elementary planning problems and search for one which best reduces the problem at hand.

Despite limitations, by visualizing local minima, we have contributed a useful algorithm to the multi-robot planning toolbox. Using this algorithm, we can increase our conceptual understanding to better debug, reduce and interact with multi-robot motion planning problems.

Bibliography

- [1] E. Artin, “Theory of braids,” *Annals of Mathematics*, pp. 101–126, 1947.
- [2] S. Bhattacharya and R. Ghrist, “Path homotopy invariants and their application to optimal trajectory planning,” *Annals of Mathematics and Artificial Intelligence*, vol. 84, no. 3-4, pp. 139–160, 2018.
- [3] Y. Diaz-Mercado and M. Egerstedt, “Multirobot mixing via braid groups,” *IEEE Transactions on Robotics*, vol. 33, no. 6, pp. 1375–1385, 2017.
- [4] A. Dobson and K. E. Bekris, “Sparse roadmap spanners for asymptotically near-optimal motion planning,” *International Journal of Robotics Research*, vol. 33, no. 1, pp. 18–47, 2014.
- [5] M. Erdmann and T. Lozano-Perez, “On multiple moving objects,” *Algorithmica*, vol. 2, no. 1-4, p. 477, 1987.
- [6] I. M. Gelfand, R. A. Silverman *et al.*, *Calculus of variations*. Courier Corporation, 2000.
- [7] W. Hönig, J. A. Preiss, T. K. S. Kumar, G. S. Sukhatme, and N. Ayanian, “Trajectory planning for quadrotor swarms,” *IEEE Transactions on Robotics*, vol. 34, no. 4, pp. 856–869, 2018.
- [8] J. E. Hopcroft, J. T. Schwartz, and M. Sharir, “On the complexity of motion planning for multiple independent objects; pspace-hardness of the” warehouseman’s problem”,” *International Journal of Robotics Research*, vol. 3, no. 4, pp. 76–88, 1984.
- [9] D. Kornhauser, G. L. Miller, and P. Spirakis, “Coordinating pebble motion on graphs, the diameter of permutation groups, and applications,” in *Symposium on the Foundations of Computer Science*. IEEE, October 1984, pp. 241–250.
- [10] S. M. LaValle, *Planning Algorithms*. Cambridge University Press, 2006.
- [11] R. Luna and K. E. Bekris, “Efficient and complete centralized multi-robot path planning,” in *IEEE International Conference on Intelligent Robots and Systems*, 2011, pp. 3268–3275.
- [12] C. I. Mavrogiannis and R. A. Knepper, “Decentralized multi-agent navigation planning with braids,” in *Workshop on the Algorithmic Foundations of Robotics*, 2016.
- [13] —, “Multi-agent trajectory prediction and generation with topological invariants enforced by hamiltonian dynamics,” in *Workshop on the Algorithmic Foundations of Robotics*, 2018.
- [14] M. Morse, *The calculus of variations in the large*, ser. Colloquium Publications. American Mathematical Society, 1934, vol. 18.
- [15] J. R. Munkres, *Topology: a first course*. Prentice-Hall, 1974.
- [16] A. Orthey and M. Toussaint, “Rapidly-exploring quotient-space trees: Motion planning using sequential simplifications,” *International Symposium of Robotics Research*, 2019.
- [17] A. Orthey, B. Frsz, and M. Toussaint, “Motion planning explorer: Visualizing local minima using a local-minima tree,” *IEEE Robotics and Automation Letters*, vol. 5, no. 2, pp. 346–353, April 2020.
- [18] E. Páll, A. Sieverling, and O. Brock, “Contingent contact-based motion planning,” in *IEEE International Conference on Intelligent Robots and Systems*. IEEE, 2018, pp. 6615–6621.

- [19] F. T. Pokorny, M. Hawasly, and S. Ramamoorthy, “Topological trajectory classification with filtrations of simplicial complexes and persistent homology,” *International Journal of Robotics Research*, vol. 35, no. 1-3, pp. 204–223, 2016.
- [20] M. Ryan, “Constraint-based multi-robot path planning,” in *IEEE International Conference on Robotics and Automation*, 2010, pp. 922–928.
- [21] T. Siméon, S. Leroy, and J. P. Laumond, “Path coordination for multiple mobile robots: A resolution-complete algorithm,” *IEEE Transactions on Robotics and Automation*, vol. 18, no. 1, pp. 42–49, 2002.
- [22] S. Smale, “On the topology of algorithms, i,” *Journal of Complexity*, vol. 3, pp. 81–89, 1987.
- [23] K. Solovey and D. Halperin, “k-color multi-robot motion planning,” *International Journal of Robotics Research*, vol. 33, no. 1, pp. 82–97, 2014.
- [24] K. Solovey, O. Salzman, and D. Halperin, “Finding a needle in an exponential haystack: Discrete RRT for exploration of implicit roadmaps in multi-robot motion planning,” *International Journal of Robotics Research*, vol. 35, no. 5, pp. 501–513, 2016.
- [25] S. Söntges and M. Althoff, “Computing possible driving corridors for automated vehicles,” *IEEE Intelligent Vehicles Symposium (IV)*, pp. 160–166, 2017.
- [26] I. A. Şucan, M. Moll, and L. Kavraki, “The open motion planning library,” *IEEE Robotics and Automation Magazine*, 2012.
- [27] P. Svestka and M. H. Overmars, “Coordinated path planning for multiple robots,” *IEEE Robotics and Autonomous Systems*, vol. 23, no. 3, pp. 125–152, 1998.
- [28] M. Toussaint and M. Lopes, “Multi-bound tree search for logic-geometric programming in cooperative manipulation domains,” in *IEEE International Conference on Robotics and Automation*, 2017, pp. 4044–4051.
- [29] J. van den Berg, J. Snoeyink, M. Lin, and D. Manocha, “Centralized path planning for multiple robots: Optimal decoupling into sequential plans,” in *Robotics: Science and Systems*, Seattle, USA, June 2009.
- [30] G. Wagner and H. Choset, “Subdimensional expansion for multirobot path planning,” *Artificial Intelligence*, vol. 219, pp. 1–24, 2015.
- [31] W. Wu, S. Bhattacharya, and A. Prorok, “Multi-Robot Path Deconfliction through Prioritization by Path Prospects,” *arXiv preprint arXiv:1908.02361*, 2019.
- [32] Y. Yang and O. Brock, “Elastic roadmaps motion generation for autonomous mobile manipulation,” *Autonomous Robots*, vol. 28, no. 1, p. 113, 2010.
- [33] J. Yu and S. M. LaValle, “Optimal multirobot path planning on graphs: Complete algorithms and effective heuristics,” *IEEE Transactions on Robotics*, vol. 32, no. 5, pp. 1163–1177, 2016.
- [34] M. Zucker, N. Ratliff, A. Dragan, M. Pivtoraiko, M. Klingensmith, C. Dellin, J. A. D. Bagnell, and S. Srinivasa, “CHOMP: Covariant Hamiltonian Optimization for Motion Planning,” *International Journal of Robotics Research*, 2013.